J. Microelectron. Packag. Soc., 23(4), 49-55 (2016) https://doi.org/10.6117/kmeps.2016.23.4.049
Print ISSN 1226-9360 Online ISSN 2287-7525

Magnetic and Thermal Evaluation of a Magnetic Tunneling Junction Current Sensor Package

Eduardo Rhod[1,†], Celso Peter[1], Willyan Hasenkamp[1] and Agner Grion[2]

[1]Electrical Engineering Graduate Program, Unisinos University, Av. Unisinos, 950 - Cristo Rei, São Leopoldo - RS, 93022-000, Brazil

[2]Science and Technology Foundation-CIENTEC, 675, Rua Washington Luiz, Rio Grande do Sul, State Government, Brazil

(Received December 5, 2016: Corrected December 19, 2016: Accepted December 23, 2016)

Abstract: Nowadays there are magnetic sensors in a wide variety of equipment such as computers, cars, airplanes, medical and industrial instruments. In many of these applications the magnetic sensors offer safe and non-invasive means of detection and are more reliable than other technologies. The electric current in a conductor generates a magnetic field detected by this type of sensor. This work aims to define a package dedicated to an electrical current sensor using a MTJ (Magnetic Tunnel Junction) as a sensing device. Four different proposals of packaging, three variations of the chip on board (CoB) package type and one variation of the thin small outline package (TSOP) were analyzed by COMSOL modeling software by simulating a brad range of current injection. The results obtained from the thermal and magnetic analysis has proven to be very important for package improvements, specially for heat dissipation performance.

Keywords: Package Design, Current Sensor, Magnetic Modeling, Thermal Modeling

1. Introduction

Magnetic sensors are a constant presence in a wide variety of equipment such as computers, cars, airplanes, medical and industrial instruments. As the electric current creates a magnetic field, according to the 4^{th} Maxwell's equation (1) which states that the magnetic field induced around a closed loop is proportional to sum of the electric current and the displacement current.

$$\nabla \times H = J_c + \frac{\partial D}{\partial t} \quad (1)$$

Reig et al. mention that even though the electric current sensing is a well established concept it is still a field that needs special instrumentation and can have limitations imposed by the traditional measurement methods. For instance, the use of shunt resistance are generally an easy and low cost method but can have significant loss and thermal limitations.[1)]

According to Arikan et al., due to new and ever growing demand for better precision and measurement range, studies in the Physics field known as spintronics has lead to the advent of new technologies like the Magnetic Tunneling Junction (MTJ).[2)] Lopes et al. states that the MTJ represents a reliable and high sensibility choice for magnetic sensing.[3)]

Reig et al. says that the design of these sensors is a delicate task and, if the sensor package is not well designed, problems like the low insulation due to wrong dielectric choice, thermal limitations due to the joule heating and mutual coupling resulting from electrical traces close to the chip sensor will likely occur.[1)] Also, according to Tummala, a package must allow that the chip performs its designed functions giving mechanical support, electrical insulation, heat dissipation and allowing the chip integration with the rest of the system.[4)] Nevertheless, the package is one of the main cost of the electronic system, according to the International Technology Roadmap for Semiconductors[5)] and need to have its costs as low as possible.

In this scenario, this work proposes a magnetic and thermal evaluation of four different options of package designs for a MTJ current sensor. Although there are several works that address the use of MTJ and other technologies for current sensing, up to the time of this article writing, there is no other work focusing on the package evaluation, especially with a complete thermal and magnetic analysis of

†Corresponding author
E-mail: ELRHOD@unisinos.br

different strategies for the package.

2. Bibliography Review

A MTJ consists of a structure composed by two ferromagnetic metal layers (electrodes), separated by an ultrathin insulating film (most of the time oxide) that acts as potential barrier, also called as tunnel barrier.[6] As a simplified understanding, the MTJ resistance is proportional to the magnetic field. This works will focus on the package aspects only. For more information regarding the MTJ sensor the reader is referred to.[7-11]

Reig et al developed a sensor in a configuration known as Wheatstone Bridge connecting the spin-valve based current sensor.[12] The authors used deposition and lithography fabrication processes to fabricate all bridge elements together to minimize the differences and lower the costs. Cubells et al. present a study of sensors using different MTJs quantities and geometrical configurations to detect current of low magnitudes.[13] The authors observed that the more devices associated, the more sensible was the resulting system and, the thinner the current conductor, the bigger the field concentration. The authors adopted the Dual Inline Package (DIP) as the sensor package.

The only work found at literature that performed computational modeling of a current sensor was the one presented by Beltran et al. in.[14] In this work the authors used Finite Element Method (FEM) simulation of the current sensor presented by Reig et al. in.[12] The authors analyzed the simulation results comparing to the previous experimental work with respect to the relation of the fabricating process parameters to the results of current, frequency and sensor positioning. The work concluded that computational model can be applied to quantify the effects caused by imperfections during the fabrication process like lateral displacements and slope deviations.

As observed from bibliography review there is a lack of publications that present package evaluation for current sensors. Therefore, present work contributes with the magnetic and thermal evaluation of four different package strategies for a current sensor.

3. Simulation Experiments

In order to evaluate which package strategy would best fit with the target sensor it is important to know what are the sensor operation parameters that need to be fulfilled. Table 1 shows the selected sensor information from Crocus Technology manufacturer.

Table 1. MTJ Sensor model Ctsr200x characteristics

Parameter	Min	Typical	Max	Unit
Voltage Supply (V_B)		3-5		V
R_{out}		1-20		kΩ
Input Bias (I_{IN})		25		mA
R_{IN}		100		Ω
Sensitivity		10		mV/mA/Oe
Linearity Range		±20		Oe
Linearity Error		1.8		%FS
Hysteresis		1.0		%FS
Max. Exposed Field		10000		Oe
Operating Frequency	DC		1000	MHz
Operating Temperature	–40		85	°C

As the 3D CAD the SolidWorks® was used as the design software to create the elements used in the simulation procedures. In order to do the FEM calculus the COMSOL® tool was the software used to solve the differential equations and calculate the thermal and magnetic solutions.

Another important definition when it comes to modeling is the materials and properties that will be considered and are necessary to describe the modeled object. In order to run the magnetic simulation it was necessary to feed the simulation tool with the material properties. Table 2 presents the electrical conductivity (σ), relative permeability (μ_r), relative permittivity (ε_r), thermal conductivity (k), thermal capacity (Cp) and density of the simulated materials.

Table 2 shows that the first column presents the main materials and compounds used in the model where Cu stands for copper, Au stands for gold, FR4 refers to the PCB compound and EMC for the epoxy mold compound.

4. Package Design and Simulation

This section presents the design of four strategies of packages and its simulation results. It is important to mention here that the main objective of proposing and simulat-

Table 2. Material properties

Mat.	Properties					
	σ	μr	εr	k	Cp	Density
	[S/m]	-	-	[W/(mK)]	[J/(kgK)]	[kg/m^3]
Cu	5.99E+7	1	1	400	385	8700
Au	4.56E+7	1	1	317	129	19300
FR4	0.0001	1	4.5	0.3	1000	1500
EMC	1.0E-12	1	4	0.63	1500	1200

ing different package strategies was to identify which one would physically have the dimensions and thermal capacity to measure a wide range of current and at the same time support the heat generated. It is important to mention here that the sensor magnetic flux and thermal limits were taken from the component datasheet.[15] The sensor magnetic flux limit values are from 0.2 mT to 220 mT while the thermal limits are from -40ºC to 85ºC. The next sessions present the simulation results for the different strategies of packages followed by brief results analysis and discussion.

4.1. Chip on Board Proposal

The first package proposal to be modeled was the so called Chip on Board (CoB). The CoB chip was composed of the main sensor and the microprocessor chip that would be responsible for the value measurement and calculations. Fig. 1 presents the full CoB package.

In order to simplify the model and run the simulation faster, the simulated version of the package was reduced to the sensor which is the interest of this work. Although the processor thermal contribution might be important, the sensor manufacturer indicates that the processor contribution can be neglected as it only does very few operations. After the package simplification the simulated chip dimensions were of 3 mm, 6 mm, 1,505 mm for length, width and high respectively, similar to presented at Fig. 3.

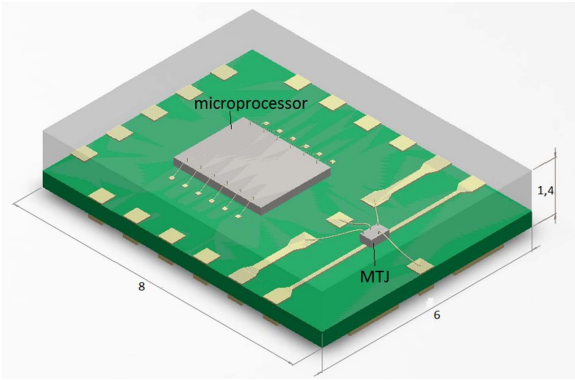

Fig. 1. Isometric view of the CoB package proposal. Dimensions in mm.

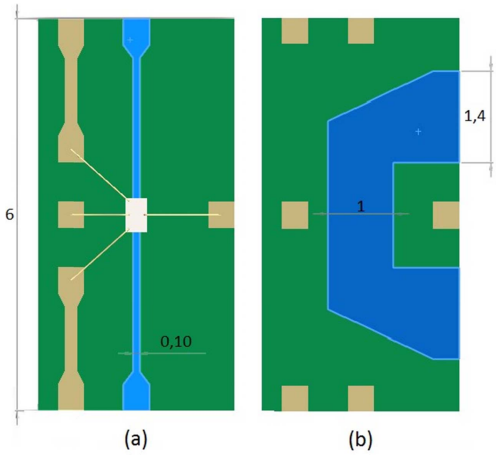

Fig. 2. CoB package proposal, top traces view (a) and bottom traces view (b). Dimensions in mm.

In this first simulation the package was designed with two copper traces positioned under the MTJ sensor with different width and thicknesses. The first of these traces (with 0.035 mm thick and 0.1 mm width) was positioned right under the sensor, at the so called top layer (Fig. 2(a)). The second one (with 0.105 mm thick and 1 mm width) was designed at the other side of the FR4 plane (0.4 mm thick), the so called bottom layer (Fig. 2(b)).

Each of the two traces were designed to support different ranges of current. The one from the top layer, with smaller section area, was simulated with 0.05A, 0.1A, 0.5A, 1A and 2A currents. The trace in the bottom, with bigger section area, was simulated with 0.5A, 1A, 2A, 3A, 5A and 10A currents. Tables 4 and 3 presents the obtained results.

Table 3 shows that, according to simulation results, only the 0.5A and 1A currents (indicated in blue color) generated values of magnetic flux and heat dissipation that are inside the established limits of 0.2 mT to 220 mT for magnetic flux and –40ºC to 85ºC of temperature range. In order to support higher currents the bottom trace was designed with bigger section area to be the path for higher current measurements. These results can be observed in Table 4.

Table 4 shows that only the 0.5A and 10A currents were

Table 3. Results for the current injection on the top trace of the CoB

Current (A)	B (DC) (mT)	B (AC) (mT)	Temp. (C)
0.05	0.045	0.045	25.15
0.1	0.089	0.089	25.59
0.5	0.446	0.446	39.63
1	0.892	0.892	83.87
2	1.784	1.784	260.88

Table 4. Results for the current injection on the bottom trace of the CoB package

Current (A)	B (DC) (mT)	B (AC) (mT)	Temp. (C)
0.5	0.121	0.121	25.41
1	0.241	0.241	26.63
2	0.483	0.483	31.53
3	0.724	0.724	39.70
5	1.207	1.207	66.05
10	2.415	2.415	189.47

out of bounds (indicated in red color). The first current value of 0.5A was too small to generate enough magnetic flux to be detected by the sensor. On the other side, the 10A generated too much heat to be supported by the sensor.

4.2. Chip on Board with Gold Wire Proposal

In this proposal the previous design was modified to allow the detection of lower currents by shortening the distance between the chip sensor and the sensed current, as it is expected that the closer to the current source, the bigger is the generated magnetic flux. As alternative, a gold wire was used as the path for lower currents and the top trace had to be redesigned to allow the gold wire routing. Fig. 3 presents the modified design with the gold wire.

Fig. 3 shows the CoB design with a gold wire of 25 μm diameter positioned 30 μm above the sensing point. The gold wire injected currents were of 0.05A, 0.1A and 0.5A. Table 5 presents the simulated results for the gold wire current injection.

Table 5 shows that the gold wire allowed the measurement for the lower currents but could not stand the high temperature imposed by the 0.5A current.

As the top trace was redesigned to allow the gold wire routing, new simulations were taken to evaluate the complete solution. Table 6 presents the obtained results.

Table 6 shows that only the 0.5A magnetic flux value was inside the magnetic and thermal limits. The new routing of the top trace imposed thermal disadvantages to the trace. As a solution to improve thermal performance, the trace was redesigned to increase the conducting area by increasing the trace dimensions. Fig. 4 presents the design changes where (a) illustrates the original trace routing from the CoB proposal, without the gold wire, (b) the CoB with the gold wire addition and (c) the CoB with the gold wire and redesign of the top trace to allow improved heat dissipation.

Table 7 presents the simulation results for the new top trace design presented in Fig. 4(c).

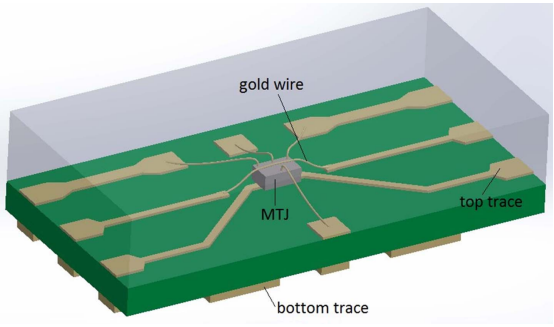

Fig. 3. Isometric view of the CoB proposal with gold wire. Dimensions in mm.

Table 5. Gold wire simulation results

Current (A)	B (DC) (mT)	B (AC) (mT)	Temp (C)
0.05	0.21	0.21	25.87
0.1	0.421	0.421	28.47
0.5	2.104	2.104	112.32

Table 6. Simulation results for the redesigned top trace

Current (A)	B (DC) (mT)	B (AC) (mT)	Temp (C)
0.05	0.045	0.045	25.17
0.1	0.090	0.090	25.68
0.5	0.448	0.448	41.98
1	0.896	0.896	93.04
2	1.791	1.791	297.16

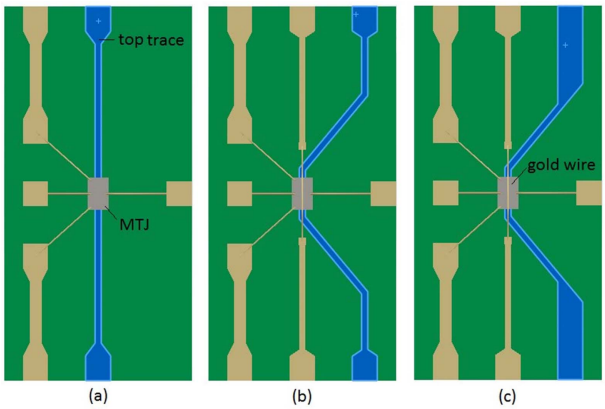

Fig. 4. Top trace simulation results for the CoB plus gold wire package proposal.

4.3. CoB Flip Chip Proposal

In this package proposal the sensor chip was considered to be assembled with the flip chip process, in which the sensor is positioned by rotating the chip 180° resulting in an inversion of the active area closer to the top trace. In

Table 7. Simulation results for top trace after design improvements

Current (A)	B (DC) (mT)	B (AC) (mT)	Temp (C)
0.05	0.044	0.044	25.13
0.1	0.087	0.087	25.50
0.5	0.436	0.436	37.47
1	0.871	0.871	74.85
2	1.743	1.743	224.29

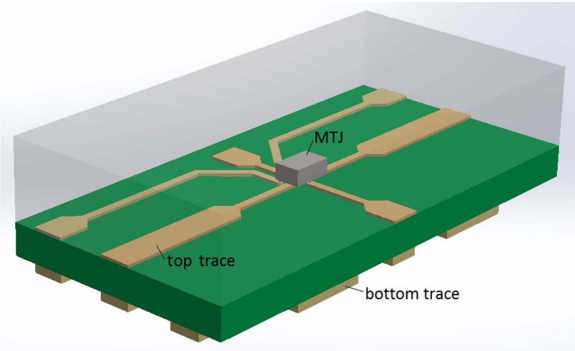

Fig. 5. Isometric view of the flip chip package strategies.

this proposal the only difference from the simulation point of view was to consider a different sensing point, much closer to the current trace. As the exact distance between the magnetic source and sensor depends on the flip chip process this study analyzed two flip chip alternatives, the *Gold Stud Bumping* and the *Electroless Ni/Au Bumping*. Fig. 5 presents the simulated isometric view.

Fig. 5 presents the resulting design for the flip chip alternatives. In this proposal the top trace was redesigned to pass as close as possible to the sensor sensing point.

In the *Gold Stud Bumping* process the ball used to connect the chip to the FR4 substrate is formed by an adaptation of the traditional gold wire process. In this case, the ball bonding is formed by using the wire bonder machine to connect the gold wire, like in the traditional wire bonding process, with the difference that after connecting the gold wire to the pad the wire bonder breaks the wire, living a bump in the shape of an inverted mushroom. This process is repeated for all pad connections. At the end, this process resulted in a distance of 30 μm from the sensing point to the magnetic source (top trace). In the *Electroless Ni/Au Bumping* process a thin Ni/Au layer is deposited over the pads to favor the flip chip connection. This process results in a thinner layer of connection which, for the simulation purposes, was considered to form a distance of 15 μm from the sensing point to the magnetic source. Table 8 presents the simulation results for both flip chip processes.

As can be observed in Table 8 the *Electroless Ni/Au Bumping* process presented a wider range of magnetic flux measurements as the sensing point is closer to the magnetic source when compared to the *Gold Stud Bumping* process. In order to evaluate bigger currents, the bottom trace was simulated and the results can be observed in Table 9.

Table 9 shows that the only value out of magnetic flux bounds for the bottom was the one resulted from the 0.5A current. When it comes to the heat dissipation, the 10A current simulation showed resulted in temperature above the established limits. Tables 8 and 9 show that the flip chip proposal was able to measure magnetic flux values for 0.1A to 5A without the need of the gold wire present at the CoB of the second proposal.

Table 8. Top trace simulating results for the CoB plus flip chip package

Current (A)	Gold Stud Bumping			Electroless Ni/Au Bumping		
	B (DC) (mT)	B (AC) (mT)	Temp (C)	B (DC) (mT)	B (AC) (mT)	Temp (C)
0.05	0.164	0.164	25.10	0.206	0.206	25.10
0.1	0.328	0.328	25.38	0.412	0.412	25.38
0.5	1.640	1.638	34.53	2.059	2.059	34.52
1	3.280	3.27	63.11	4.118	4.118	63.29
2	6.561	6.554	177.70	8.236	8.236	178.43

Table 9. Simulation results for the CoB flip chip package proposal for currents injected at the bottom trace

Current (A)	Gold Stud Bumping			Electroless Ni/Au Bumping		
	B (DC) (mT)	B (AC) (mT)	Temp (C)	B (DC) (mT)	B (AC) (mT)	Temp (C)
0.5	0.149	0.149	25.42	0.152	0.152	25.42
1	0.298	0.298	26.67	0.305	0.305	26.67
2	0.596	0.596	31.68	0.609	0.609	31.68
3	0.894	0.894	40.02	0.914	0.914	40.03
5	1.490	1.490	66.73	1.523	1.523	66.74
10	2.980	2.980	192.20	3.046	3.046	192.22

4.4. Thin Small Outline Package - TSOP Proposal

The fourth package proposal is based on the Thin Small Outline Package - TSOP, which is a thinner variation of the Small Outline Package - SOP. The designed TSOP was based on the JEDEC standard (DG-4.15B).[16] Fig. 6 presents the designed TSOP package proposal with a gold wire to measure low magnitude currents.

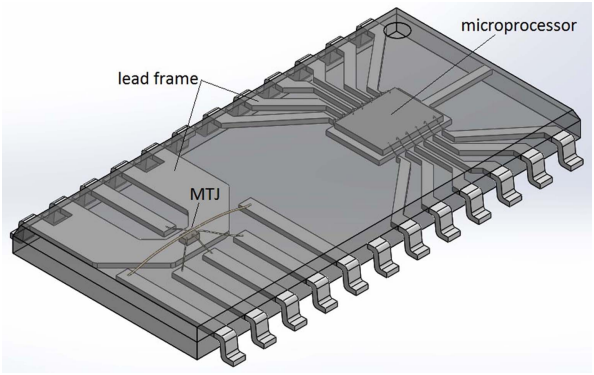

Fig. 6. Isometric view of the complete TSOP package solution.

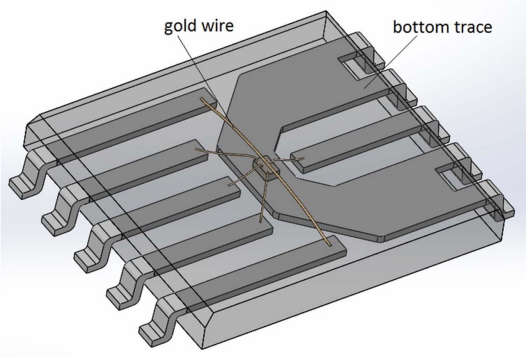

Fig. 7. Isometric view of the simulated TSOP package solution.

In order to reduce the model complexity and simulation time without compromising the simulation results, the design from Fig. 6 was simplified by removing the microprocessor area. Fig. 7 presents the simplified version that was obtained and used at simulation procedures.

In the design, the trace under the sensor chip has 1mm width and 180 μm thickness. As for the gold wire, the resulting wire length is 5.08 mm positioned 30 μm above the sensor with two different diameters, 50 μm and 25 μm. The main difference between the TSOP solution to the other package strategies is the use of the lead frame as the current path instead of PCB traces. Simulation results are presented in Table 10.

When analyzing the simulation results from Table 10 one may conclude that there is a error in the magnetic flux presented for both wires with the same current. As the magnetic flux is proportional to the injected current even if there is different current densities, there should be no difference in the results of Table 10 for the same injected currents. This difference can be explained as, with the increase in the diameter, the center of the gold wire was displaced for the smaller diameter wire in comparison to the bigger one. To put in numbers, the gold wire with 25 μm diameter had its center positioned 42.5 μm above the sensor, while in the 50 μm diameter case the center of the wire was positioned 55 μm above (12.5 μm difference). This difference resulted in the values presented in Table 10 and was enough to generate results inside the limit range for the 0.05A with 25 μm diameter wire, but became outside of the range for the same current for the 50 μm wire, as the wire center was displaced 12.5 μm away of the sensor. On the other hand, the wire with bigger diameter supported higher currents which can be explained as, the bigger the wire diameter, the higher the supported temperature.

Table 10. Simulation results for the TSOP package solution for the gold wire injections

Current (A)	Wire diameter of 25 μm			Wire diameter of 50 μm		
	B (DC) (mT)	B (AC) (mT)	Temp (C)	B (DC) (mT)	B (AC) (mT)	Temp (C)
0.05	0.223	0.223	25.70	0.167	0.167	25.11
0.1	0.446	0.446	27.88	0.335	0.335	25.45
0.5	2.232	2.232	97.52	1.673	1.673	36.69
1	4.464	4.464	315.06	3.346	3.346	71.74
2	8.928	8.928	1185.20	6.691	6.691	212.21

Table 11. Simulation results for the lead frame current injections

Current (A)	B (DC) (mT)	B (AC) (mT)	Temp (C)
0.5	0.206	0.206	25.15
1	0.412	0.412	25.59
2	0.824	0.824	27.46
3	1.236	1.236	30.53
5	2.060	2.060	40.45
10	4.120	4.120	86.87

The next simulation experiment evaluated the lead frame trace for the different values of current. Table 11 presents the obtained simulation results. When comparing the results from Table 11 to the ones obtained from previous designs simulations, one can notice a significant increase in the results of the magnetic flux range for almost all current ranges. That happened because there was the FR4 substrate between the sensor element and trace in the previous simulations. Also when comparing the temperature results for all the current range, one can observe a significant decrease in the temperature value for all the current range. That happened because the lead frame is thicker than the bottom copper trace of the CoB solutions. Even though the resulted temperature for 10A current was higher that the accepted limit. In order to improve heat dissipation and support the measurement of up to 10A currents, the TSOP

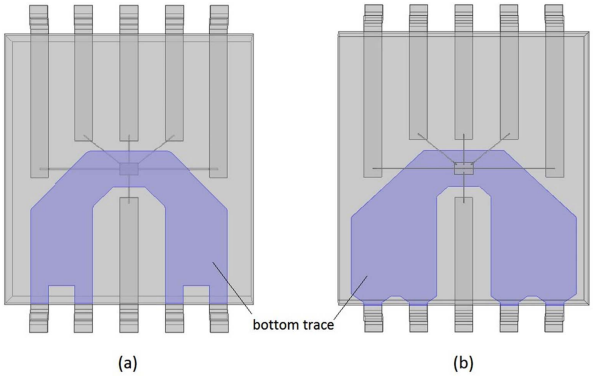

Fig. 8. Lead frame modifications to improve thermal performance (a) original and (b) modified.

Table 12. Simulation results for the modified bottom trace of the TSOP package type

Current (A)	B (DC) (mT)	B (AC) (mT)	Temp (C)
0.5	0.206	0.206	25.13
1	0.411	0.411	25.52
2	0.822	0.822	27.13
3	1.233	1.233	29.80
5	2.055	2.055	38.41
10	4.110	4.110	78.63

design was modified by increasing the lead frame area as can be seen in Fig. 8.

Fig. 8(a) shows the original lead frame design and (b) the new lead frame design to support wider current ranges. Simulation results of the new design are presented at Table 12.

Table 12 shows that the sensor presented measurement values inside the working range for all the injected current values. Even for the 10A current the observed simulated temperature was around 79°C, which is bellow the sensor limit of 85°C.

5. Conclusions and Future Work

Table 13 summarizes the four package proposals with respect to the range of current that each proposal was able to measure regarding the magnetic flux and temperature limits established by the sensor manufacturer.

From Table 13, presented above, one can conclude that all proposals but the first CoB one could be the selected package type for the current sensor of this work. Although simulation results were not validated with experimental measurements the four solutions here proposed started with simple simulation models found in literature. This work demonstrates the importance of the simulation modeling phase in the design of new packages. Specially for thermal improvements, simulation results indicated that there were space for design improvements that lead to significant increase in the package thermal dissipation capacity.

Table 13. Summary of the current ranges supported by each package proposal

Package Proposal	Current Range
CoB	0.5A to 5A
CoB + Gold Wire	0.05A to 5A
CoB + Flip Chip	0.05A to 5A
TSOP	0.1A to 10A

References

1. C. Reig, M.-D. Cubells-Beltran and D. Ramırez, “Magnetic field sensors based on giant magnetoresistance (GMR) technology: Applications in electrical current sensing”, Sensors, 9(10), 7919 (2009).
2. M. Arikan, S. Ingvarsson, M. Carter and G. Xiao, “Dc and ac characterization of mgo magnetic tunnel junction sensors”, IEEE Transactions on Magnetics, 49(11), 5469 (2013).
3. A. Lopes, S. Cardoso, R. Ferreira, E. Paz, F. L. Deepak, J. Sanchez, D. Ramírez, S. I. Ravelo and P. P. Freitas, “Mgo magnetic tunnel junction electrical current sensor with integrated ru thermal sensor”, IEEE Transactions on Magnetics, 49(7), 3866 (2013).
4. R. R. Tummala, “Fundamentals of microsystems packaging”, McGraw-Hill Professional, (2001).
5. L. Wilson, International technology roadmap for semiconductors (ITRS), Assembly and packaging, (2011).
6. S. Yuasa, “Tunneling magnetoresistance: Experiment (mgo magnetic tunnel junctions)”, Handb. Spin Transp. Magn., CRC Press, Boca Raton., 217 (2012).
7. P. R. LeClair and J. S. Moodera, “Tunneling magnetoresistance: Experiment (non-mgo magnetic tunnel junctions)”, Handb. Spin Transp. Magn., CRC Press, Boca Raton., 197 (2012).
8. W. Y. Du, “Resistive, capacitive, inductive, and magnetic sensor technologies”, CRC Press, (2014).
9. G. Xiao, “Magnetoresistive sensors based on magnetic tunneling junctions”, Handb. Spin Transp. Magn., CRC Press, Boca Raton., 665 (2012).
10. S. Yuasa and D. D. Djayaprawira, “Giant tunnel magnetoresistance in magnetic tunnel junctions with a crystalline MgO(001) barrier”, Journal of Physics D: Applied Physics, 40(21), R337 (2007).
11. J. Zhu and C. Park, “Magnetic tunnel junctions”, Materials Today, 9(11), 36 (2006).
12. C. Reig, D. Ram´ırez, F. Silva, J. Bernardo and P. Freitas, “Design, fabrication, and analysis of a spinvalve based current sensor”, Sensors and Actuators, A: Physical, 115(2), 259 (2004).
13. M. D. Cubells, C. Reig, A. De Marcellis, A. Roldan, J. B. Roldan, S. Cardoso and P. P. Freitas, “Magnetic tunnel junction (mtj) sensors for integrated circuits (ic) electric current measurement”, Proc. IEEE SENSORS 2013 (2013).
14. H. Beltran, C. Reig, V. Fuster, D. Ramírez and M. D. Cubells-Beltran, “Modeling of magnetoresistive-based electrical current sensors: A technological approach”, IEEE Sensors Journal, 7(11) 1532 (2007).
15. Crocus, Product brief ctsr200x series. Last access: Jan. (2014), http://www.crocus-technology.com
16. J. D. Standard, “Design requirements for outlines of solid state and related products”, Joint Electron Device Engineering Council - JEDEC, 13 (2004).